How to cite: *Angew. Chem. Int. Ed.* **2024**, *63*, e202319235
doi.org/10.1002/anie.202319235

Homochirality

RNA-Templated Peptide Bond Formation Promotes L-Homochirality

Ewa Węgrzyn[+], Ivana Mejdrová[+], Felix M. Müller, Milda Nainytė, Luis Escobar, and Thomas Carell**

Abstract: The world in which we live is homochiral. The ribose units that form the backbone of DNA and RNA are all D-configured and the encoded amino acids that comprise the proteins of all living species feature an all-L-configuration at the α-carbon atoms. The homochirality of α-amino acids is essential for folding of the peptides into well-defined and functional 3D structures and the homochirality of D-ribose is crucial for helix formation and base-pairing. The question of why nature uses only encoded L-α-amino acids is not understood. Herein, we show that an RNA-peptide world, in which peptides grow on RNAs constructed from D-ribose, leads to the self-selection of homo-L-peptides, which provides a possible explanation for the homo-D-ribose and homo-L-amino acid combination seen in nature.

Introduction

Folding of peptides into well-defined and functional protein structures,[1,2,3] as well as the duplex formation of RNA and DNA,[4,5,6] in which information can be stored due to Watson-Crick base-pairing,[7] requires homochirality.[8,9] The living nature that surrounds us evolved based on homo-D-configured ribose, which forms the backbone of RNA and DNA, and homo-L-configured α-amino acids, which are indispensable in the world of proteins. While homochirality is the prerequisite for folding of these biopolymers into 3D structures, the question of why D-sugars are combined with L-amino acids and not with the D-counterparts and hence the diastereoselectivity of nature is unknown.[10,11,12]

[*] E. Węgrzyn,[+] Dr. I. Mejdrová,[+] Dr. F. M. Müller, Dr. M. Nainytė, Dr. L. Escobar, Prof. Dr. T. Carell
Department of Chemistry, Institute for Chemical Epigenetics (ICE-M)
Ludwig-Maximilians-Universität (LMU) München
Butenandtstrasse 5-13, 81377 Munich (Germany)
E-mail: luisescobar1992@hotmail.es
thomas.carell@lmu.de

[+] These authors contributed equally.

The current idea of how life may have started is based on the RNA world hypothesis, in which RNAs self-replicated and folded into catalytically active structures.[13,14,15] At some point in evolution, these RNA structures gained the potential to connect amino acids to form peptides and proteins with increasing catalytic capabilities.[16] Even though there is more than one model to explain how RNA learned, at some point, to make peptides and proteins, the amino acids were initially likely connected to each other in close proximity to the RNA structures, with RNAs acting as peptide forming catalysts.

We recently reported the idea that, instead of a pure RNA world, chimeric RNA-amino acid/peptide structures may have created an RNA-peptide world, in which RNA and peptides were covalently connected until the structures got large enough to replace covalent bonding by non-covalent interactions.[17,18,19] We observed that RNA strands equipped with ubiquitous non-canonical nucleosides, such as 5-methylaminomethyl uridine (mnm^5U) and threonine-modified N^6-carbamoyl adenosine (Thr^6A), which are found in contemporary transfer RNAs (tRNAs)[20,21,22] and which can be considered to be molecular fossils,[23,24] allow RNA to self-decorate with peptides.[18]

The synthesis cycle that allows peptides to form directly on RNA is depicted in Figure 1a, but it should be mentioned again that this is just one example of how peptides can be formed on and by RNA. The key features of our model involve: 1. the reaction of two amino acids, attached via the non-canonical nucleosides m^6aa^6A and mnm^5U to complementary RNA strands, to give a stable hairpin structure. 2. The subsequent cleavage of the urea bond by simple heating, which breaks the hairpin. This is followed by a potential exchange (3. release/4. annealing) of the formed m^6A-containing donor RNA strand for another amino acid-containing oligonucleotide. Repeating this cycle allows the growing of longer peptides on the acceptor RNA strand.

Although it is impossible to prove that these particular reactions were indeed involved in creating an RNA-peptide world on the early Earth, it is a prebiotically plausible concept of how RNA could have initially templated the synthesis of peptides. The models of how RNA encoded peptide synthesis have in common that the peptide forming reactions take place on RNA. Consequently, our non-canonical nucleoside-based model allows us to investigate the stereochemical preferences of RNA-templated peptide growth.

Previous studies by the research groups of Lacey,[25,26] Tamura and Schimmel,[27,28,29,30,31] Sutherland[32,33,34] and

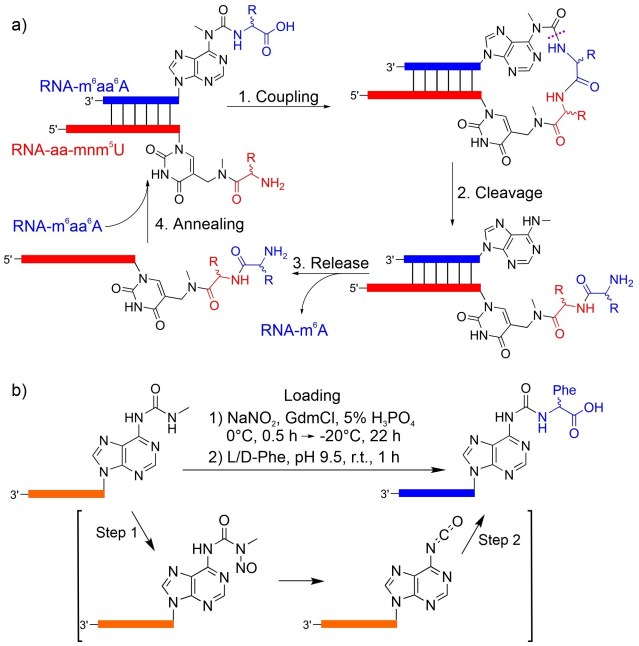

Figure 1. a) RNA-peptide synthesis cycle involving donor and acceptor RNA strands with m^6aa^6A and aa-mnm^5U, respectively, and b) prebiotic loading reaction of a racemic mixture of L/D-Phe onto an RNA strand containing a terminal N^6-methylcarbamoyl adenosine nucleotide. GdmCl = guanidinium chloride.

Richert[35] showed already that α-amino acids connected to 5'-phosphorylated nucleotides and RNAs, either via the carboxylic acid group as acyl phosphate mixed anhydrides,[36] or with the α-amino group in the form of phosphoramidates,[37] react preferentially when they are L-configured. Herein, we investigated how our RNA-peptide synthesis cycle (Figure 1a) is influenced by stereochemistry.

Results and Discussion

The first step of the RNA-templated peptide growth cycle involves the loading of an amino acid onto the donor RNA strand to give a non-canonical amino acid-modified adenosine nucleotide, $(m^6)aa^6A$. For example, Gly^6A and $(m^6)Thr^6A$ are known to exist in the anticodon loop of contemporary tRNAs.[38,39,40,41] Previously, we showed that this loading step could be achieved in a prebiotically plausible way by the reaction of an N^6-methylurea adenosine nucleotide with NO^+ in the presence of amino acids or even peptides via an N^6-isocyanate intermediate (Figure 1b).[19,42] Therefore, we initially investigated whether the loading reaction displayed any stereochemical preference. We performed this reaction onto an RNA strand containing an N^6-methylcarbamoyl adenosine nucleotide at the 5'-end with a racemic mixture of L/D-Phe. The aromatic amino acid was chosen because it facilitates the analysis of this crude reaction mixture by high-performance liquid chromatography (HPLC) using UV/Vis detection. In this loading reaction, we did not observe any stereochemical preference (Figure S12). The L- and D-Phe were loaded onto the RNA strand with the same preference, which gives a 1:1 isomeric mixture of the terminal L- and D-Phe^6A nucleotides in 35 % overall yield.

We next investigated how the peptide growth reaction (step 1, Figure 1a) is influenced by either L- or D-amino acids. For these experiments, we synthesized a series of donor and acceptor RNA strands (**ON1** and **ON2**, respectively) using an automated solid-phase RNA synthesizer and 2'-OMe nucleosides (Figure 2 and SI). We used the 2'-OMe nucleosides, which are very prevalent in contemporary ribosomal RNA (rRNA), to increase the stability of the phosphodiester backbone toward hydrolysis and to achieve higher duplex melting temperatures with short RNA strands.[43,44,45] In particular, we prepared the 7-mer donor RNA strands **ON1a-e** with either L- and D-amino acid-modified N^6-methylcarbamoyl adenosine nucleotides ($m^6aa^6A_m$) at the 5'-end. We also synthesized the complementary 11-mer acceptor RNA strands **ON2a** with either L- and D-amino acid-modified 5-methylaminomethyl uridine nucleotides (aa-mnm^5U_m) at the 3'-end. We focused at Val, Ala and Thr, which are thought to have been early amino acids. They are found in meteorites and they are formed under prebiotically plausible conditions.[46,47,48,49,50,51,52,53] All RNA strands were purified by HPLC and characterized by matrix-assisted laser desorption/ionization time-of-flight (MALDI-TOF) mass spectrometry (MS) (Tables S1-S2).

Next, peptide formation reactions leading to the corresponding hairpin intermediates were performed (Figure 2). In order to enable accurate analysis of the stereochemical outcome of the coupling reactions by HPLC, we first synthesized independently the hairpins **ON3a-e** as standards from the complementary donor and acceptor RNA strands **ON1a-e** and **ON2a**. After annealing of **ON1a-e** with **ON2a**, we added in each case 50 mM of an activator,[54] either 1-

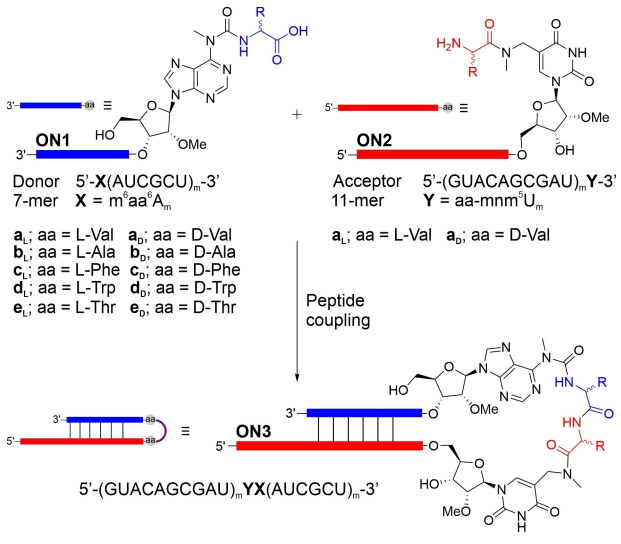

Figure 2. Peptide coupling reactions between donor and acceptor RNA strands, **ON1** and **ON2**, respectively, to yield hairpin products, **ON3**. The RNA strands used in this work contained L- and D-amino acids. aa = amino acid and R = aa side chain. m (subscript) indicates that the RNA strands were composed of 2'-OMe nucleotides.

ethyl-3-(3-dimethylaminopropyl) carbodiimide with *N*-hydroxysulfosuccinimide (EDC/Sulfo-NHS) or 4-(4,6-dimethoxy-1,3,5-triazin-2-yl)-4-methylmorpholinium chloride (DMTMM•Cl), in 100 mM 2-(*N*-morpholino)ethanesulfonate (MES) buffer at pH 6 containing 100 mM of NaCl. After 2-6 h at r.t., the obtained hairpin reference compounds **ON3a-e** were isolated by HPLC and characterized by MALDI-TOF MS (Table S3).

With these standards in hand, we next investigated the diastereoselectivity of the RNA-based peptide synthesis (Figure 2). To this end, we studied the coupling of the donor RNA strands **ON1**, connected to either an L- (**ON1$_L$**) or a D-amino acid (**ON1$_D$**), with the complementary acceptor RNA strands **ON2**, containing either an L-Val (**ON2a$_L$**) or a D-Val (**ON2a$_D$**), in direct competition experiments (Figure 3a-c). First, we started with Val in the donor RNA strand **ON1a**. For the experiment, we prepared an equimolar solution of **ON1a$_L$** (L-Val) and **ON1a$_D$** (D-Val) in water. HPLC analysis of the mixture confirmed the 1:1 relationship (Figure 3a). Next, we performed the peptide coupling reaction after the addition of 1 equiv. of the acceptor RNA strand **ON2a$_L$** (L-Val) using the activator EDC/Sulfo-NHS (MES buffer pH 6, NaCl, r.t., 2 h). HPLC analysis of the crude reaction mixture revealed the formation of the two possible hairpin products, **ON3a$_{LL}$** (L-Val,L-Val) and **ON3a$_{DL}$** (D-Val,L-Val), in 69 % overall yield (Figure 3b). To our surprise, we immediately noted a significant selectivity for the L,L-product. **ON3a$_{LL}$** formed with a remarkable diastereoselectivity of 93:7 (L,L:D,L). For comparison, we carried out the same competition experiment (**ON1a$_L$** and **ON1a$_D$**) in the presence of the acceptor RNA strand **ON2a$_D$** (D-Val). In this case, the HPLC analysis showed a lower yield for **ON3a$_{LD}$** (L-Val,D-Val) plus **ON3a$_{DD}$** (D-Val,D-Val) of only 36 % and a lower diastereoselectivity of only 66:34 (L,D:D,D) (Figure 3c). Similar results were obtained when we repeated the competition experiments with **ON1a** and **ON2a** at lower temperature (5 °C, Table S9). These data showed that the L,L-hairpin products are the preferred reaction outcomes. If we assume that life started with the formation of peptides close to RNA, we can surmise that the D-ribose in RNA promotes L-homochirality of the peptide formed in close proximity.

To further strengthen this argument, we repeated the experiment with other amino acids using the L/D-donor

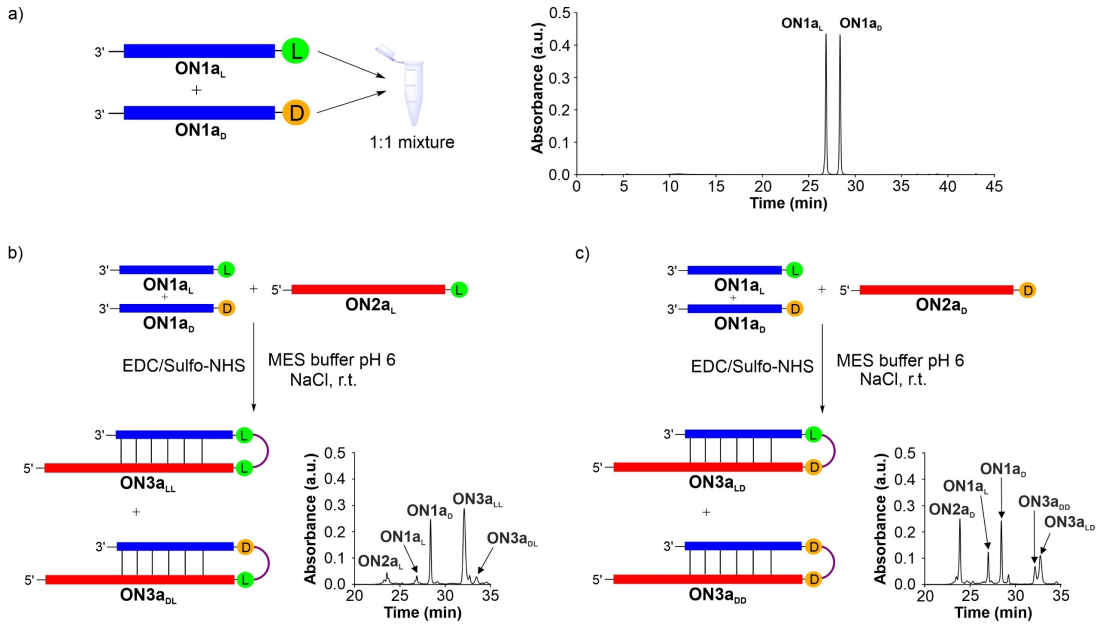

L,L + D,L combination

Donor strands	Acceptor strand	Overall yield (%)	[ON3$_{LL}$]/[ON3$_{DL}$] ratio
ON1a$_L$ + ON1a$_D$		69 (90)	93:7 (58:42)
ON1b$_L$ + ON1b$_D$		72 (85)	80:20 (70:30)
ON1c$_L$ + ON1c$_D$	ON2a$_L$	61 (99)	86:14 (77:23)
ON1d$_L$ + ON1d$_D$		74 (99)	n.d.
ON1e$_L$ + ON1e$_D$		73 (84)	91:9 (70:30)

L,D + D,D combination

Donor strands	Acceptor strand	Overall yield (%)	[ON3$_{LD}$]/[ON3$_{DD}$] ratio
ON1a$_L$ + ON1a$_D$		36 (90)	66:34 (41:59)
ON1b$_L$ + ON1b$_D$		55 (88)	52:48 (50:50)
ON1c$_L$ + ON1c$_D$	ON2a$_D$	40 (99)	29:71 (52:48)
ON1d$_L$ + ON1d$_D$		48 (99)	38:62 (50:50)
ON1e$_L$ + ON1e$_D$		65 (84)	71:29 (47:53)

Figure 3. a) Equimolar mixture of **ON1a$_L$** and **ON1a$_D$**, and competitive peptide coupling reactions between **ON1a$_L$** and **ON1a$_D$** with: b) **ON2a$_L$** and c) **ON2a$_D$**. The HPLC chromatograms correspond to the analyzed crude reaction mixtures and the tables summarize the results obtained for the coupling reactions of **ON1a-e** and **ON2a** using EDC/Sulfo-NHS and DMTMM•Cl (in parenthesis) as activators. n.d. = not determined due to product overlap. Reaction conditions: [**ON1**] = 50 μM; [**ON2**] = 50 μM; [buffer] = 100 mM; [NaCl] = 100 mM and [activator] = 50 mM. Yields determined by HPLC analysis using the calibration curve of a reference compound (Figure S2).

RNA strands **ON1b-e** loaded with Ala, Phe, Trp and Thr (Figure 3 and Figures S4-S5). The competition experiments with the acceptor RNA strands, **ON2a$_L$** and **ON2a$_D$**, provided, in all cases, the expected hairpin products **ON3b-e**. Again, with EDC/Sulfo-NHS activator, we observed better yields with **ON2a$_L$** (61-74 %) compared to the reaction with **ON2a$_D$** (40-65 %). For the L,L:D,L-selectivity using **ON2a$_L$**, we measured diastereoselectivities from 80:20 (L,L:D,L, **ON1b**) to 91:9 (L,L:D,L, **ON1e**) (Figure 4a). In contrast, turning the selectivity experiment around (L,D:D,D-combinations) with the acceptor strand **ON2a$_D$**, bearing a D-amino acid, provided unpredictable and largely fluctuating selectivities ranging from 29:71 (L,D:D,D, **ON1c**) to 71:29 (L,D:D,D, **ON1e**) (Figure 4b).

When we changed the activation method to DMTMM•Cl, we observed diastereoselectivities from 58:42 (L,L:D,L, **ON1a**) to 77:23 (L,L:D,L, **ON1c**) for the preferred L:D,L-combinations with **ON2a$_L$** and only ca. 50:50 (L,D:D,D) mixtures for the L:D,D-combinations with **ON2a$_D$** (Figure 3b-c). In all cases, the L,L-combinations with **ON2a$_L$** gave high yields and better diastereoselectivities.

We next wanted to know whether these selectivities change when we use a prebiotically more suitable activation method and performed experiments with methyl isonitrile (MeNC) in 4,5-dicyanoimidazole (DCI) buffer at pH 6.[55] We observed in the experiments with selected donor RNA strands, **ON1b** (Ala) and **ON1c** (Phe), the clean formation of the hairpin products **ON3b-c** in less than 16 % overall yield (Table S6). However, the diastereoselectivities were very high with >72 % in favor of the homochiral dipeptide products. Only for the competitive reactions with the acceptor RNA strand **ON2a$_D$**, we obtained different diastereoselectivity ratios for the same amino acid depending on the activator used (EDC/Sulfo-NHS, DMTMM•Cl or MeNC).

In order to study how the selectivities evolve when larger peptides grow on RNA, we next prepared donor RNA strands containing L-homochiral di- and tripeptides with Val, **ON1f$_L$** and **ON1g$_L$**, respectively (see SI). In the first set of competition experiments with the activator EDC/Sulfo-NHS, we used an equimolar mixture of **ON1a$_L$** with **ON1f$_L$** or **ON1g$_L$** (Figure 5a and Figure S7). The competitive coupling reactions with **ON2a$_L$** indicated that the mono-L-Val donor RNA strand **ON1a$_L$** reacted preferentially with the acceptor strand to give the L,L-dipeptide hairpin **ON3a$_{LL}$** with high selectivities of 73:27 and 89:11 over the larger tri- and tetrapeptide hairpin products, **ON3f$_{LL}$** and **ON3g$_{LL}$**. In contrast, the same competition reactions with the acceptor strand carrying a D-amino acid, **ON2a$_D$**, showed low selectivity (ca. 50:50).

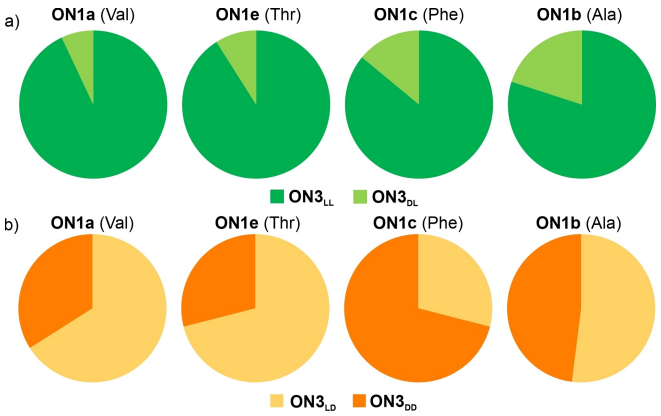

Figure 4. Relative isomeric composition of the hairpin products, **ON3**, obtained in the competitive peptide coupling reactions between **ON1** with: a) **ON2a$_L$** and b) **ON2a$_D$**.

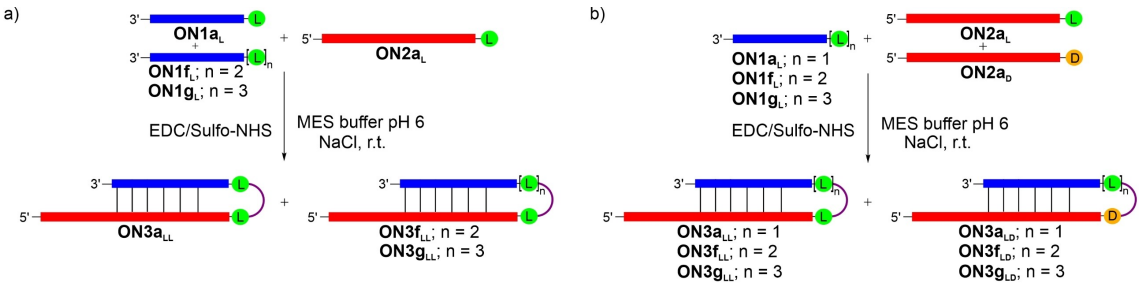

Donor strands	Acceptor strand	Overall yield (%)	[ON3a$_{LL}$]/[ON3f,g$_{LL}$] ratio
ON1a$_L$ + ON1f$_L$	ON2a$_L$	79	73:27
ON1a$_L$ + ON1g$_L$		71	89:11
Donor strands	**Acceptor strand**	**Overall yield (%)**	**[ON3a$_{LD}$]/[ON3f,g$_{LD}$] ratio**
ON1a$_L$ + ON1f$_L$	ON2a$_D$	49	51:49
ON1a$_L$ + ON1g$_L$		33	58:42

Donor strand	Acceptor strands	Overall yield (%)	[ON3$_{LL}$]/[ON3$_{LD}$] ratio
ON1a$_L$	ON2a$_L$ + ON2a$_D$	73	87:13
ON1f$_L$		54	66:34
ON1g$_L$		32	67:33

Figure 5. Competitive peptide coupling reactions a) between **ON2a$_L$** with **ON1a$_L$** and **ON1 f,g$_L$**, and b) between **ON2a$_L$** and **ON2a$_D$** with **ON1a$_L$**, **ON1f$_L$** or **ON1g$_L$**. The tables summarize the results obtained using EDC/Sulfo-NHS as activator. All amino acids and peptides contain Val. Reaction conditions: [**ON1**] = 50 μM; [**ON2**] = 50 μM; [buffer] = 100 mM; [NaCl] = 100 mM and [activator] = 50 mM. Yields determined by HPLC analysis using the calibration curve of a reference compound (Figure S2).

In a second set of experiments, we conducted reverse competition reactions with the activator EDC/Sulfo-NHS, in which an equimolar mixture of **ON2a$_L$** and **ON2a$_D$** was allowed to couple with either **ON1a$_L$**, **ON1f$_L$** or **ON1g$_L$** (Figure 5b and Figure S8, see SI for a competition experiment with **ON1a$_D$**). In all these cases, the results showed a clear preference for the formation of the L,L-homochiral products **ON3$_{LL}$**. The highest diastereoselectivity was obtained with the mono-L-Val donor RNA strand **ON1a$_L$** (87:13 L,L:L,D). The longer di- and tripeptides in **ON1f$_L$** and **ON1g$_L$** led to decreased selectivities of 66:34 and 67:33 (L,L:L,D), respectively. All together, these data suggest a strong tendency for the preferred formation of L-homochiral peptides, when the peptide synthesis occurs in close proximity to RNA.

In order to investigate whether the tendency to grow all-L-homochiral peptides is the result of different thermodynamic stabilities of the initially formed RNA duplexes, we measured melting temperatures (T_m) and we determined rate constants (k_{app}) for the peptide coupling reactions using selected donor and acceptor RNA strands. For reasons of prebiotic plausibility, we decided to perform these experiments with the amino acid Val in **ON1a** and **ON2a**, respectively.

First, we measured the melting temperatures of all possible duplex combinations (**ON1a$_L$**•**ON2a$_L$**, **ON1a$_D$**•**ON2a$_L$**, **ON1a$_L$**•**ON2a$_D$** and **ON1a$_D$**•**ON2a$_D$**) using temperature-dependent UV spectroscopy experiments at 260 nm (Figure 6a). All recorded melting curves displayed a mono-sigmoidal shape and were fit to a two-state model.[56] The obtained data showed that the T_m values were indistinguishable for the four donor•acceptor RNA duplex combinations with $T_m = 37.1 \pm 0.8$ °C. In addition, we measured the same T_m value for an RNA duplex composed of **ON1a$_L$** and **ON2b**, which lacked the amino acid at the 3'-terminal mnm^{5}U nucleotide (Figure 6a). These data showed that different duplex stabilities cannot explain the observed diastereoselectivities.

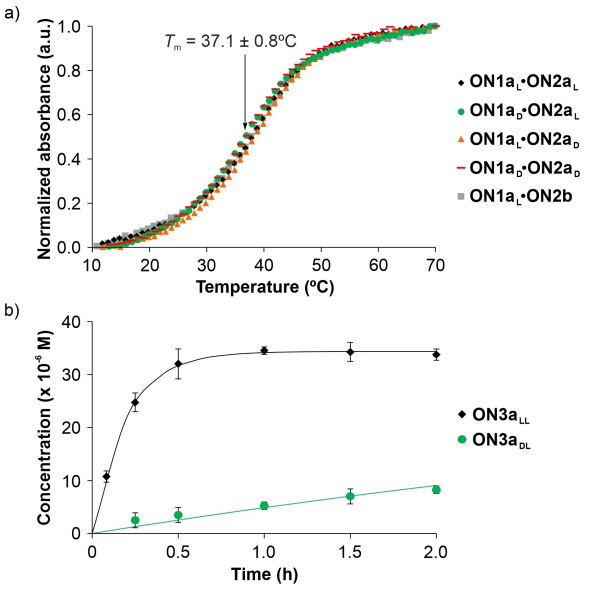

Figure 6. a) UV (260 nm) melting curves of the four possible duplexes formed between the donor RNA strands **ON1a$_L$** and **ON1a$_D$** with the acceptor RNA strands **ON2a$_L$** and **ON2a$_D$**. The melting curve of **ON1a$_L$** with **ON2b** (acceptor RNA strand without amino acid) is also shown. b) Kinetic plots for the separate peptide coupling reactions of **ON2a$_L$** with **ON1a$_L$** and **ON1a$_D$**, respectively, using EDC/Sulfo-NHS as activator. Error bars are shown as standard deviations.

To determine the rate constants, we monitored separate peptide coupling reactions between the complementary donor and acceptor RNA strands at different time intervals using EDC/Sulfo-NHS (Figure 6b and Figure S10) and DMTMM•Cl (Figures S9-S10) as activators. The kinetic data for the formation of the hairpin products (**ON3a$_{LL}$**, **ON3a$_{DL}$**, **ON3a$_{LD}$** and **ON3a$_{DD}$**) were fit to a pseudo-first order equation[57] (see SI). The calculated apparent rate constant values were, as expected, different and dependent on the donor RNA strand, **ON1a$_L$** and **ON1a$_D$**, as well as the activator used (Table 1). To our delight, we noted that the hairpin product ratios, calculated using exclusively the k_{app} values (k_{app} (**ON1a$_L$**)/k_{app} (**ON1a$_D$**) = [**ON3a$_L$**]/[**ON3$_D$**]), are in good agreement with the values obtained in the competition experiments (Figure 3b-c). Taken together, these data support the idea that the L-amino acids are better aligned for reaction on RNA (constructed from D-ribose). The D-ribose creates a right-handed A-form RNA helix that appears to promote L-homochirality if the amino acids react directly on the RNA to form peptides.

Conclusions

Nature utilizes homo-D-ribose to build the backbone of DNA and RNA and homo-L-configured α-amino acids to create well-defined and functional protein structures. Herein, we investigated the question of how RNA can help to

Table 1: Apparent rate constant values (k_{app}) determined for the peptide coupling reactions of **ON1a** with **ON2a** using EDC/Sulfo-NHS and DMTMM•Cl as activators. Errors are indicated as standard deviations.

Activator	Donor strand	Acceptor strand	Hairpin strand	k_{app} (h^{-1})	Calcd. ratio[a]
EDC/ Sulfo-NHS	**ON1a$_L$**	**ON2a$_L$**	**ON3a$_{LL}$**	5.04 ± 0.12	87
	ON1a$_D$		**ON3a$_{DL}$**	0.15 ± 0.01	13
	ON1a$_L$	**ON2a$_D$**	**ON3a$_{LD}$**	n.d.	n.d.
	ON1a$_D$		**ON3a$_{DD}$**	0.32 ± 0.01	n.d.
DMTMM•Cl	**ON1a$_L$**	**ON2a$_L$**	**ON3a$_{LL}$**	0.91 ± 0.07	59
	ON1a$_D$		**ON3a$_{DL}$**	0.43 ± 0.01	41
	ON1a$_L$	**ON2a$_D$**	**ON3a$_{LD}$**	0.54 ± 0.01	47
	ON1a$_D$		**ON3a$_{DD}$**	0.68 ± 0.03	53

[a] Product ratio calculated from the measured apparent rate constants. n.d. = not determined due to signal overlap with activated species.

establish an L-homochiral peptide world. The basic assumption was that initially peptides were formed close to RNA or directly connected to RNA in an RNA-peptide world. To simulate this process, we used our recently introduced concept of peptide growth directly on RNA as a model.[18]

First, we studied the stereochemical preference of the loading reaction of an amino acid onto RNA. We observed that this reaction provided donor RNA strands with a 1:1 relationship of the L- and D-amino acids. Specifically, we studied how L/D-Phe reacts with an RNA strand, equipped with a terminal N^6-methylcarbamoyl adenosine nucleotide, which creates in situ an N^6-isocyanate. Both L- and D-amino acids reacted with the same preference and hence no diastereoselectivity was observed. Next, we investigated the coupling reaction with a set of selected amino acids (Val, Ala, Phe, Trp and Thr), and we observed a high preference for the coupling of L-configured amino acids connected to RNAs. In all cases, we found that the L,L-homochiral dipeptide hairpin products were formed in better yields and with higher diastereoselectivities. This preference was maintained even when larger tri- and tetrapeptide hairpins, for the growth of longer peptides, were formed. On the other hand, the coupling reactions with a D-amino acid on the acceptor RNA strand provided variable selectivities depending on the amino acid and the activator, potentially because of an unfavorable steric alignment of the amino acids for coupling.

These data allow us to formulate a scenario that yields an all-L-homochiral peptide world. If we assume that small RNAs (or nucleosides) captured amino acids and peptides out of the primordial soup to bring them in close proximity within an RNA duplex, the connection of the amino acids to each other is strongly favored when the amino acids are L-configured, which leads with time to an enrichment of the L,L-coupling products. Repetitive cycles of peptide growth and peptide release followed by recapturing of the peptides by RNA and connection of the recaptured peptides with either amino acids or peptides could then lead to a possible outgrowth process that provides a homo-L-configured peptide world.

What it is next needed is a scenario that leads to the preferred recapturing of peptides over single amino acids and fragment condensation reactions, which were already observed,[18] that quickly grow longer peptide structures in just a few chemical steps.

The most important result of this study is that D-ribose-based nucleotides, which give rise to right-handed A-form RNA duplexes, preferentially connect L-amino acids to form homo-L-peptides. We do not address in this study the question of the origin of homo-D-RNA.

Supporting Information

Reaction procedures, characterization data, peptide coupling reactions, melting curves, kinetic experiments and additional references are included in the Supporting Information (Ref. [17,18,19,56,57,58,59,60,61,62,63]).

Acknowledgements

We thank the Deutsche Forschungsgemeinschaft for supporting this research through the DFG grants: CA275/11-3 (ID: 326039064), CRC1309 (ID: 325871075, A4), CRC1032 (ID: 201269156, A5) and CRC1361 (ID: 393547839, P2). We thank the Volkswagen Foundation for funding this research (grant EvoRib). This project has received funding from the European Research Council (ERC) under the European Union's Horizon 2020 research and innovation program under grant agreement No. 741912 (EPiR). L. E. thanks the Alexander von Humboldt Foundation for a postdoctoral fellowship (ESP 1214218 HFST-P). Open Access funding enabled and organized by Projekt DEAL.

Conflict of Interest

The authors declare no conflict of interest.

Data Availability Statement

The data that support the findings of this study are available in the supplementary material of this article.

Keywords: Amino Acids · Diastereoselectivity · Homochirality · RNA-Peptide World · Origin of Life

[1] C. M. Dobson, *Nature* **2003**, *426*, 884–890.
[2] D. Balchin, M. Hayer-Hartl, F. U. Hartl, *Science* **2016**, *353*, aac4354.
[3] B. Kuhlman, P. Bradley, *Nat. Rev. Mol. Cell Biol.* **2019**, *20*, 681–697.
[4] R. E. Dickerson, H. R. Drew, B. N. Conner, R. M. Wing, A. V. Fratini, M. L. Kopka, *Science* **1982**, *216*, 475–485.
[5] P. Belmont, J.-F. Constant, M. Demeunynck, *Chem. Soc. Rev.* **2001**, *30*, 70–81.
[6] A. Travers, G. Muskhelishvili, *FEBS J.* **2015**, *282*, 2279–2295.
[7] J. D. Watson, F. H. C. Crick, *Nature* **1953**, *171*, 737–738.
[8] W. A. Bonner, N. E. Blair, F. M. Dirbas, *Origins Life Evol. Biospheres* **1981**, *11*, 119–134.
[9] K. Tamura, *J. Mol. Evol.* **2019**, *87*, 143–146.
[10] S. Toxvaerd, *Int. J. Mol. Sci.* **2009**, *10*, 1290–1299.
[11] S. F. Ozturk, D. D. Sasselov, *Proc. Natl. Acad. Sci. USA* **2022**, *119*, e2204765119.
[12] S. F. Ozturk, Z. Liu, J. D. Sutherland, D. D. Sasselov, *Sci. Adv.* **2023**, *9*, eadg8274.
[13] L. E. Orgel, *J. Mol. Biol.* **1968**, *38*, 381–393.
[14] W. Gilbert, *Nature* **1986**, *319*, 618.
[15] G. F. Joyce, *Nature* **2002**, *418*, 214–221.
[16] J. C. Bowman, N. V. Hud, L. D. Williams, *J. Mol. Evol.* **2015**, *80*, 143–161.
[17] M. Nainytė, F. Müller, G. Ganazzoli, C.-Y. Chan, A. Crisp, D. Globisch, T. Carell, *Chem. Eur. J.* **2020**, *26*, 14856–14860.
[18] F. Müller, L. Escobar, F. Xu, E. Węgrzyn, M. Nainytė, T. Amatov, C. Y. Chan, A. Pichler, T. Carell, *Nature* **2022**, *605*, 279–284.
[19] J. N. Singer, F. M. Müller, E. Węgrzyn, C. Hölzl, H. Hurmiz, C. Liu, L. Escobar, T. Carell, *Angew. Chem. Int. Ed.* **2023**, *62*, e202302360.
[20] P. F. Agris, *Nucleic Acids Res.* **2004**, *32*, 223–238.

[21] T. Carell, C. Brandmayr, A. Hienzsch, M. Muller, D. Pearson, V. Reiter, I. Thoma, P. Thumbs, M. Wagner, *Angew. Chem. Int. Ed.* **2012**, *51*, 7110–7131.
[22] H. Grosjean, E. Westhof, *Nucleic Acids Res.* **2016**, *44*, 8020–8040.
[23] M. P. Robertson, S. L. Miller, *Science* **1995**, *268*, 702–705.
[24] M. Di Giulio, *J. Theor. Biol.* **1998**, *191*, 191–196.
[25] J. C. Lacey, R. D. Thomas, M. P. Staves, C. L. Watkins, *Biochim. Biophys. Acta Protein Struct. Mol. Enzymol.* **1991**, *1076*, 395–400.
[26] N. S. M. D. Wickramasinghe, M. P. Staves, J. C. Lacey Jr., *Biochemistry* **1991**, *30*, 2768–2772.
[27] K. Tamura, P. Schimmel, *Science* **2004**, *305*, 1253.
[28] K. Tamura, P. R. Schimmel, *Proc. Natl. Acad. Sci. USA* **2006**, *103*, 13750–13752.
[29] K. Tamura, *BioSystems* **2008**, *92*, 91–98.
[30] K. Tamura, *Int. J. Mol. Sci.* **2011**, *12*, 4745–4757.
[31] K. Tamura, *Life* **2015**, *5*, 1687–1699.
[32] L.-F. Wu, M. Su, Z. Liu, S. J. Bjork, J. D. Sutherland, *J. Am. Chem. Soc.* **2021**, *143*, 11836–11842.
[33] S. J. Roberts, Z. Liu, J. D. Sutherland, *J. Am. Chem. Soc.* **2022**, *144*, 4254–4259.
[34] M. Su, C. Schmitt, Z. Liu, S. J. Roberts, K. C. Liu, K. Röder, A. Jäschke, D. J. Wales, J. D. Sutherland, *J. Am. Chem. Soc.* **2023**, *145*, 15971–15980.
[35] O. Doppleb, J. Bremer, M. Bechthold, C. Sánchez Rico, D. Göhringer, H. Griesser, C. Richert, *Chem. Eur. J.* **2021**, *27*, 13544–13551.
[36] S. A. Kauffman, N. Lehman, *Interface Focus* **2023**, *13*, 20230009.
[37] J. J. Petkowski, W. Bains, S. Seager, *Molecules* **2019**, *24*, 866.
[38] G. B. Chheda, R. H. Hall, D. I. Magrath, J. Mozejko, M. P. Schweizer, L. Stasiuk, P. R. Taylor, *Biochemistry* **1969**, *8*, 3278–3282.
[39] M. P. Schweizer, K. McGrath, L. Baczynskyj, *Biochem. Biophys. Res. Commun.* **1970**, *40*, 1046–1052.
[40] F. Kimura-Harada, D. L. Von Minden, J. A. McCloskey, S. Nishimura, *Biochemistry* **1972**, *11*, 3910–3915.
[41] L. Perrochia, E. Crozat, A. Hecker, W. Zhang, J. Bareille, B. Collinet, H. van Tilbeurgh, P. Forterre, T. Basta, *Nucleic Acids Res.* **2013**, *41*, 1953–1964.
[42] C. Schneider, S. Becker, H. Okamura, A. Crisp, T. Amatov, M. Stadlmeier, T. Carell, *Angew. Chem. Int. Ed.* **2018**, *57*, 5943–5946.
[43] L. L. Cummins, S. R. Owens, L. M. Risen, E. A. Lesnik, S. M. Freier, D. McGee, C. J. Guinosso, P. D. Cook, *Nucleic Acids Res.* **1995**, *23*, 2019–2024.
[44] S. M. Freier, K.-H. Altmann, *Nucleic Acids Res.* **1997**, *25*, 4429–4443.
[45] W. A. Decatur, M. J. Fournier, *Trends Biochem. Sci.* **2002**, *27*, 344–351.
[46] L. M. Longo, J. Lee, M. Blaber, *Proc. Natl. Acad. Sci. USA* **2013**, *110*, 2135–2139.
[47] S. L. Miller, H. C. Urey, *Science* **1959**, *130*, 245–251.
[48] D. Ring, Y. Wolman, N. Friedmann, S. L. Miller, *Proc. Natl. Acad. Sci. USA* **1972**, *69*, 765–768.
[49] Y. Wolman, W. J. Haverland, S. L. Miller, *Proc. Natl. Acad. Sci. USA* **1972**, *69*, 809–811.
[50] C. Huber, G. Wächtershäuser, *Science* **2006**, *314*, 630–632.
[51] L. M. Longo, M. Blaber, *Arch. Biochem. Biophys.* **2012**, *526*, 16–21.
[52] M. Kimura, S. Akanuma, *J. Mol. Evol.* **2020**, *88*, 372–381.
[53] R. Root-Bernstein, A. G. Baker, T. Rhinesmith, M. Turke, J. Huber, A. W. Brown, *Life* **2023**, *13*, 265.
[54] Z. J. Gartner, M. W. Kanan, D. R. Liu, *Angew. Chem. Int. Ed.* **2002**, *41*, 1796–1800.
[55] Z. Liu, L.-F. Wu, J. Xu, C. Bonfio, D. A. Russell, J. D. Sutherland, *Nat. Chem.* **2020**, *12*, 1023–1028.
[56] S. G. J. Mochrie, *Am. J. Phys.* **2011**, *79*, 1121–1126.
[57] S. Hoops, S. Sahle, R. Gauges, C. Lee, J. Pahle, N. Simus, M. Singhal, L. Xu, P. Mendes, U. Kummer, *Bioinformatics* **2006**, *22*, 3067–3074.
[58] F. Himmelsbach, B. S. Schulz, T. Trichtinger, R. Charubala, W. Pfleiderer, *Tetrahedron* **1984**, *40*, 59–72.
[59] F. Ferreira, F. Morvan, *Nucleosides Nucleotides Nucleic Acids* **2005**, *24*, 1009–1013.
[60] A. V. Tataurov, Y. You, R. Owczarzy, *Biophys. Chem.* **2008**, *133*, 66–70.
[61] G. R. Fulmer, A. J. M. Miller, N. H. Sherden, H. E. Gottlieb, A. Nudelman, B. M. Stoltz, J. E. Bercaw, K. I. Goldberg, *Organometallics* **2010**, *29*, 2176–2179.
[62] X. Li, J. Wu, X. Li, W. Mu, X. Liu, Y. Jin, W. Xu, Y. Zhang, *Bioorg. Med. Chem.* **2015**, *23*, 6258–6270.
[63] D. L. Usanov, A. I. Chan, J. P. Maianti, D. R. Liu, *Nat. Chem.* **2018**, *10*, 704–714.

Manuscript received: December 13, 2023
Accepted manuscript online: February 26, 2024
Version of record online: April 5, 2024